Improving our Understanding of Hantaviruses: A Multidisciplinary Approach
Stevie Fawcett, Spring 2024

Stephanie N. Seifert, PhD

Assistant Professor
Paul G. Allen School for Global Health
College of Veterinary Medicine
Washington State University
Office: 509-335-3831
Email: stephanie.seifert@wsu.edu

Table of Contents

Introduction……pg 4
General characteristics of hantaviruses……pg 4
New World hantaviruses……..pg 6
Old World hantaviruses……pg 8
Objective……pg 9

Part One: Medicine ……pg 10
Background……pg 10
Methods……..pg 11
Results……pg 11
Conclusion……..pg 14

Part Two: Epidemiology……pg 15
Background……pg 15
Methods……..pg 17
Results……pg 19
Conclusion……..pg 19

Part Three: Molecular Biology……pg 21
Background……pg 21
Methods……..pg 22
Results……pg 25
Conclusion……pg 32

Acknowledgements……pg 33

References……pg 34

List of Figures

Figure 1: Reported cases of hantavirus infection in the United States – pg 7

Figure 2: Currently recognized symptoms of hantavirus infection – pg 12

Figure 3: Sky view of the selected sites for rodent sampling – pg 18

Figure 4: Portion of seropositive rodents in natural/agroecosystem landscapes – pg 20

Figure 5: Visual representation of VSV pseudo type production – pg 24

Figure 6: Images of cells isolated from *P. maniculatus* – *pg 26*

Figure 7: Images of cells isolated from *C. perspicillata* – pg 26

Figure 8: Characteristics of novel cell lines derived from *P. maniculatus* - pg 27

Figure 9: Characteristics of novel cell lines derived from *C. perspicillata – pg 27*

Figure 10: Viral entry phenotypes on primary cells derived from *P. maniculatus – pg 29*

Figure 11: Viral entry phenotypes on primary cells derived from *C. perspicillata – pg 29*

Figure 12: Viral entry phenotypes on immortalized cells from *C. perspicillata – pg 29*

Figure 13: Growth curve of Sin Nombre virus CDC isolate on novel cell lines – pg 30

Figure 14: Growth curve of Sin Nombre virus field sample on novel cell lines – pg 31

Figure 15: Hantaan virus CPE in immortalized *Carollia perspicillata* – pg 32

Introduction

General Characteristics of Hantaviruses

Orthohantaviruses (hantaviruses) are a diverse group of viruses that can be found anywhere in the world. There are two main groups of hantaviruses: New World hantaviruses, which are found in the Americas, and Old World hantaviruses, which are mostly found in Europe and Asia. Many of these viruses are classified as zoonotic pathogens and are typically transmitted by rodent species, although there is increasing evidence that these viruses may circulate in multiple other taxa, including the orders *Chiroptera* and *Soricomorpha* (1*).* While most zoonotic hantaviruses are thought to pose little risk of onward transmission in humans, there is some evidence that Andes virus, a hantavirus found in South America, has the ability to be transmitted between humans (2). Hantaviruses pose a major threat to global health and are considered by many as potential pandemic pathogens. Importantly, there is also evidence that hantavirus-related disease may increase due to climate change and its impacts (3).

At the molecular level, hantaviruses are enveloped, segmented, negative sense, single stranded RNA viruses, about 80-120 nanometers in diameter (4). The hantavirus genome is made of three RNA segments, named small (S), medium (M), and large (L). Viral infection is mediated by the hantavirus Gn/Gc glycoproteins, which are encoded by the M segment. Hantaviruses typically target endothelial cells and have the largest impact on lung and kidney tissue. In humans, beta integrins and DAF/CD55 have been identified as potential receptors for all hantavirus types. However, protocadherin 1 has recently been identified as an essential component in virus entry for New World

hantaviruses as well (5). Hantavirus receptors in reservoir species have not been identified.

Hantaviruses are known to cause two distinct disease types: hantavirus cardiopulmonary syndrome (HCPS) and hemorrhagic fever with renal syndrome (HFRS). New World hantaviruses, such as Sin Nombre virus and Andes virus, cause HCPS, while Old World hantaviruses like Hantaan virus and Seoul virus cause HFRS. Hantaviruses have an incubation period of 1-8 weeks (6), after which they start to cause initial symptoms. Hantavirus infections primarily present with high fever, headache, hypotension, and abdominal pain for about seven days. This first stage is similar in both New World and Old World hantavirus infections.

In cases of HFRS, there are many associated secondary symptoms that vary by virus type. For example, blurred vision is associated with Puumala virus, while internal bleeding is more associated with Dobrava and Hantaan virus. The most common symptoms during the second phase of HFRS, termed the oliguric phase, are decreased urine production, acute kidney injury (marked by increases in serum creatine and urea), and bradycardia. HFRS-associated mortality is associated with organ failure, renal insufficiency, or septic shock. In cases of HCPS, the secondary phase is called the cardiopulmonary phase, which is characterized by cough, elevated heart rate, breathing irregularities, and severe hypotension. Death from HCPS is usually caused by pulmonary edema or septic shock. In both HCPS and HFRS, thrombocytopenia is a common indicator of hantavirus infection, and can be indicative of disease severity (7).

New World Hantaviruses

The most common New World hantaviruses are Sin Nombre virus in North America and Andes virus in South America, both of which cause hantavirus cardiopulmonary syndrome (HCPS) and have a mortality rate between 40% and 50%. Although the first major outbreak in the Americas occurred more than 30 years ago, there are still no treatments or vaccines for New World hantaviruses. This is mostly due to the fact that hantaviruses are severely understudied in many areas of the world. For example, in several countries in South and Central America, very little is known about hantavirus infections, despite many New World hantaviruses circulating in South and Central American countries. In fact, hantavirus publications during the last 40 years have mainly been produced by the United States, China, and Europe (8), even though South America may have a higher disease burden, indicated by its 25 hantavirus genotypes and many reservoir species (9). Besides Andes virus, other New World hantaviruses that have been found in South and Central America include Playa do Oro virus in Mexico, Choclo virus in Panama, Laguna Negra virus in Argentina/Panama/Bolivia, Araraquara virus in Brazil, Rio Mamore virus in Bolivia/Peru, and Oran virus in Argentina (10). These viruses are maintained in nature by several different rodent species, most of which belong to the *Oligoryzomys* genus. However, hantaviruses have also been detected in several species of bats in Brazil (11), including *Carollia perspicillata* (Seba's short-tailed bat), which has been shown to harbor Araraquara virus (12).

In the United States, Sin Nombre virus is the most common New World hantavirus, causing approximately 20-50 total reported cases of HCPS every year (6) (Figure 1). This virus circulates in *Peromyscus maniculatus* (the North American deer mouse), and is transmitted via respiration of feces, urine, or saliva of the reservoir species. Because deer mice are the transmission vectors for this virus, HCPS is also more commonly reported in Western and Midwestern states, where deer mice are most often found. There are also several other pathogenic New World hantaviruses that have been found in the United States, including New York virus, Black Creek Canal virus, and Bayou virus.

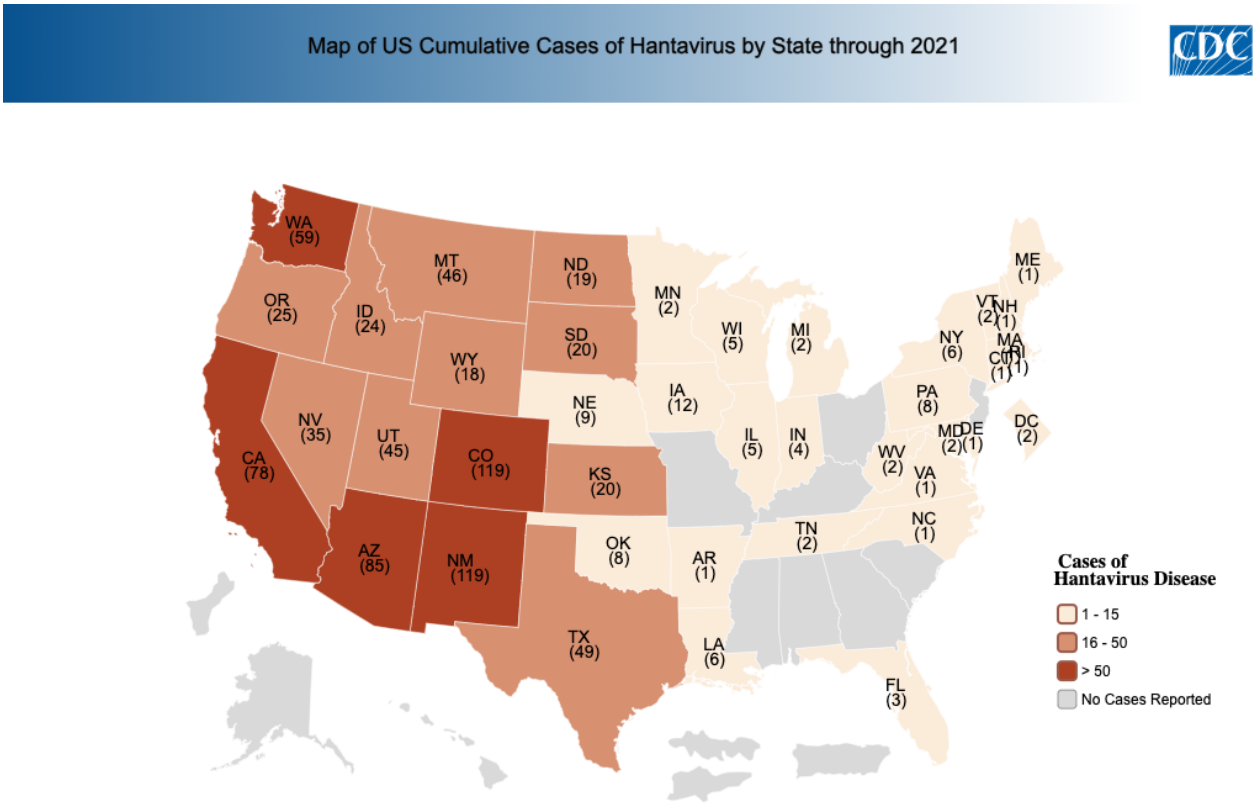

Figure 1: Reported cases of hantavirus infection in the United States 1993-2021 (cdc.gov)

Old World Hantaviruses

Old World hantaviruses are less deadly than New World hantaviruses, with mortality rates between 1% and 15% (13). However, these viruses are more widespread and are responsible for a greater number of infections. In fact, Old World hantaviruses are responsible for hundreds of thousands of infections annually across Europe, Africa, and Asia (7). Hantaan virus, which was the first hantavirus to be discovered in 1976, is now responsible for the most hantavirus infections worldwide. This virus is currently found across Korea, China, and Russia. Puumala virus, Dobrava virus, and Amur virus are also known to cause significant disease in Europe and Western Asia. Seoul virus, another Old World virus, is the only hantavirus found worldwide. Like New World hantaviruses, Old World hantaviruses are harbored and transmitted by several species of rodents, including mice, rats, and voles. There is also evidence that hantaviruses across Africa and Asia are harbored by bat and shrew species (14).

Unlike New World hantaviruses, there are several Old World hantavirus vaccines that are used in China and Korea. The first vaccine was developed against Hantaan virus in Korea, and is derived from inactivated virus particles. Despite its ability to induce seroconversion in human patients, this vaccine has shown limited capacity to protect against hantavirus disease progression. China also uses an inactivated virus vaccine for Hantaan virus and Seoul virus. These vaccines have been shown to be effective and induce immunity for up to 33 months (15).

Objective

Although our understanding of hantaviruses has improved in recent years, our knowledge of these pathogens is still very limited. More specifically, hantavirus research needs to be improved in three main areas: medicine, epidemiology, and molecular biology. In medicine, many hantavirus infections are not diagnosed or reported due to poor physician awareness. Because hantavirus infections can have a broad range of presenting symptoms, these infections are not often tested for, and can be misdiagnosed or missed entirely. In order to develop better systems for reporting and treating hantavirus infections, it is essential that health care workers are trained on the risk factors, vulnerable population demographics, and full range of symptoms associated with hantavirus infections. Secondly, it is essential that we conduct research to locate and track reservoir species for hantaviruses. The first step in disease prevention is risk reduction, and managing disease vectors for these viruses could serve as an important tool for reducing disease transmission and preparing local public health systems for potential outbreaks. Lastly, advancing our understanding of the hantavirus life cycle and virus-host interactions is an important step in developing vaccines and treatments for hantavirus-related diseases. One significant obstacle we currently face in this area is a lack of *in vitro* tools for hantavirus research. In particular, the lack of suitable cell lines for laboratory work has hindered out ability to study hantaviruses in conditions that mimic its natural state in reservoir species. Developing these cell lines would fill a major gap in this research and equip researchers the tools they need to create preventative vaccines and treatment options for hantavirus infections. In this report, I review and summarize multiple research projects that seek to

improve our understanding of hantaviruses in medicine, epidemiology, and molecular biology.

Part One: Expanding the Criteria for Hantavirus Symptomatology in Medicine

Background

Despite the longstanding surveillance of HCPS as a reportable, communicable disease in the United States, there are several crucial aspects of hantavirus infection and clinical presentation that remain poorly understood. Outside the United States, many countries do not have surveillance systems to track hantavirus infections, so the lack of information regarding hantavirus symptomatology and prevalence is even more pronounced. In recent years, there has been increasing evidence that the presenting symptoms of hantavirus infections may be more diverse than originally thought. Additionally, it is likely that many cases of HCPS and HFRS are misdiagnosed or unreported, due to lack of physician awareness, and limited access to medical are in rural communities where hantavirus-related diseases are most common.

Historically, hantavirus infections are associated with flu-like symptoms (such as headache, fever, myalgia, abdominal pain, back pain, joint pain, and nausea), followed by progressive respiratory distress in cases of HCPS and renal dysfunction or failure in cases of HFRS. In some cases, both the lungs and the kidneys may be impacted at the same time (16). However, in the last few years there has also been mounting evidence that hantaviruses may affect other organ systems outside the renal and respiratory system.

Methods

To investigate the typical symptoms that physicians associate with hantaviruses, five practicing physicians were interviewed regarding the markers they recognize as indicative of a hantavirus infection. Subsequently, a literature review was conducted to gather information on atypical symptomatology that has previously been reported for hantavirus infections. This review summarizes several different medical case reports that cited instances of hantavirus infections primarily affecting the liver, heart, and central nervous system. Finally, recommendations were formulated with the goal of improving the recognition and treatment of hantavirus infections.

Results

During interviews, practicing physicians reported symptoms associated with hantavirus infections that were consistent with the literature and consisted mainly of thrombocytopenia, fever, headache, hemoconcentration, respiratory failure, and renal failure (Figure 2). However, these physicians also indicated that they had very little experience with confirmed cases of hantavirus infections, which remains a major barrier to improved knowledge of hantavirus-related diseases. Many indicated that because of the non-specific, mild nature of the initial symptoms hantaviruses cause, they would be unlikely to test for hantavirus unless symptoms worsen. In some cases, they may also recommend against hospitalization. Notably, infectious diseases specialists were the most familiar with the clinical features of hantaviruses infection.

Physician specialty	Location of practices	Identified symptoms
Pulmonology	Salt Lake City Utah, Bend Oregon	Thrombocytopenia, pulmonary edema, capillary leakage, internal bleeding, hemoconcentration, leukocytosis
Infectious Diseases	Dartmouth New Hampshire, Bend Oregon	Thrombocytopenia, fever, renal failure, bleeding, clotting, shock, cough, respiratory failure
Internal Medicine	Salem Oregon, Redmond Oregon, Bend Oregon	If patient does not improve after 24-48 hours in hospital, impaired pulmonary and renal function, call in specialists
Infectious Diseases	Denver Colorado, Iowa City Iowa, Sioux Falls South Dakota, Bend Oregon	Fever, shortness of breath, cough, hemoconcentration, thrombocytopenia, headache, myalgia
Infectious Diseases, Internal Medicine	Bend Oregon, Fresno California, Oklahoma City Oklahoma	Fever, respiratory distress, radiographic abnormalities, hemoconcentration, thrombocytopenia, lymphocytosis

Figure 2: Recognized symptoms of hantavirus infection, as reported by practicing physicians in pulmonology, infectious disease, and internal medicine.

Atypical Symptoms Associated with Hantavirus Infections

Hepatic Manifestations

Old World hantaviruses have been shown to cause damage to the liver, although this is typically in conjunction with renal manifestations. However, in some cases hepatitis has been the primary symptom in hantavirus infection (16). Additionally, hantavirus infection has been shown to exacerbate autoimmune cholangitis, which typically results in disrupted bile flow and jaundice (17). These findings are likely due to the immune response to hantavirus infection, rather than the infection itself. This presentation is easily confused with other infections, such as hepatitis virus infections and leptospirosis (15).

Cardiac Manifestations

Cardiac involvement in Old World hantavirus infections is well documented but not well recognized. Bradycardia (18) and myocarditis (19) are the most common cardiac symptoms associated with hantavirus infections, and may present as the primary symptom in many cases following an unspecific phase, especially when the causative agent is Puumala virus. Generally, cardiac involvement in hantavirus infections is thought to be related to vascular leakage in pulmonary vessels. This leakage leads to increased pulmonary pressure and cardiac distress (20).

Neurological symptoms

Perhaps the most important pathophysiological effect of hantavirus infections apart from typical pulmonary and renal manifestations is the impact these viruses have on the brain. Although it is not commonly reported, there have been many cases of hantavirus infections with neurological involvement. These cases include instances of encephalitis (25) (26), blurred vision (21), vertigo (22), central nervous system (CNS) lesions (23) (24), acute encephalopathy (27), epileptic seizures (28), and Guillain-Barre Syndrome (29). Although most neurological manifestations have been reported in instances of Old World hantavirus infections, both New World and Old World hantaviruses have been found to impact the nervous system. Nervous system involvement is often reported in conjunction with pulmonary and renal manifestations, but not always.

Puumala virus has been found to impact the CNS quite frequently, although the associated symptoms are usually mild, such as headache, vertigo, and blurred vision. More severe symptoms include confusion, spontaneous loss of vision, seizures, and CNS hemorrhage (24). Seoul virus has also been known to cause CNS hemorrhage, in addition to viral encephalitis (25), (26). Several suspected Hantaan virus infections in China have also been complicated by neurological symptoms similar to those observed in Puumala virus infections, and seizures have been reported in cases of Dobrava virus infection (27). For New World hantaviruses, Andes virus has been shown to cause encephalitis in rare instances (28), and Sin Nombre virus has been linked to cases of seizures, spinal cord edema, and severe altered mental status both in the presence and absence of pulmonary manifestations (29), (30).

Neurological symptoms have also been reported after patients have recovered from hantavirus infections. In some cases in the United States, survivors of HCPS have shown cognitive impairment up to one year after recovering from infection (31). Additionally, several patients with Old World hantavirus infections have developed Guillen-Barre syndrome after infection. This syndrome has resulted in muscle weakness, back pain, and numbness in the chest, abdomen, and extremities (32).

Conclusion

Although the surveyed physicians were generally aware of the symptoms associated with HCPS and HFRS, they did not appear to have any knowledge of hepatic, cardiac, or neurological symptoms associated with hantavirus infections. In areas where instances of hantavirus infection are particularly prevalent, this may result

in missed diagnoses and underestimated reporting. In turn, this hinders efforts to reduce risk factors associated with hantavirus infection and reduces the amount of information available to the public related to hantavirus transmission and presentation. Therefore, it is vital that practicing physicians in multiple specialties are informed about atypical hantavirus symptomatology, particularly in areas where hantaviruses and their disease vectors are known to be present.

Part Two: Studying Factors that Influence Hantavirus Epidemiology in the Palouse

Background

Hantaviruses cause one to five cases of reported HCPS every year in Washington, and about one annual case of reported HCPS in Idaho (6). This disease has been documented in the Palouse grassland ecoregion (Palouse) for several decades and has caused severe disease and mortality in both Eastern Washington and Western Idaho (34), (35), (36). This is mainly due to the presence of the North American deer mouse (*Peromyscus maniculatus*), a known generalist rodent and synanthropic species in the Palouse that harbors Sin Nombre virus. It is known that Sin Nombre virus can be contracted from deer mice excrement, such as urine, feces, or saliva. However, the epidemiological risk factors associated with hantavirus transmission is limited, particularly for the deer mouse, in anthropogenic landscapes. Thus, we performed a case-study in the Palouse grassland ecoregion.

The Palouse is an agricultural ecosystem (agroecosystem) which depends heavily on agriculture, and consists of crop farms, cattle ranches, and natural areas. Because of this, many areas of the Palouse have been transformed into

agroecosystems, which are known to be an important aspect of anthropogenic land use, as they provide resources for both humans and wildlife. Although deer mice are known to live in several different environments, they are especially well-adapted to domestic environments and often share spaces with humans due to their synanthropic behavior (33). This creates opportunities for contact with humans and increases the risk for zoonotic disease spillover (37). Additionally, agroecosystems can provide resources for rodent populations, such as food and protection from predators. This can lead to higher population densities in agricultural centers (38), which have also been found to harbor populations of deer mice with higher hantavirus seroprevalence than that of mice living in native habitats (39). These relationships suggest that landscape types in the Palouse region may have an impact on deer mice populations and hantavirus distribution.

Generally, hantavirus epidemiology is poorly understood, which has made it difficult to elucidate the factors that contribute to virus circulation and shedding in native rodent populations. This is a large obstacle that prevents us from identifying vulnerable communities and adjusting local public health systems to better recognize and treat hantavirus infections. Because the Palouse region is heavily dependent on agriculture, it is important to understand how these activities can influence rodent populations and hantavirus circulation. Studying how human-modified areas of the Palouse landscape may reveal drivers of rodent abundance and is the first step to understand the potential of zoonotic spillover in this region.

Methods

Sites in Eastern Washington and Western Idaho were selected for sampling based on the density of native landscape surrounding them. This study was conducted over the course of two summers. During the first summer, a total of seven sites were selected. Catherine Grady et al, later expanded this to fourteen sites in 2023. Although all sampling areas included cattle and crop farms, the sites in Western Idaho were more connected to natural forest than the sites in Eastern Washington. This method of site selection utilized a block design, where similar groups of sites were sampled in two geographic areas that differed only in their connection to native landscapes (Figure 3). This strategy allowed us to study the effect of agricultural areas on rodent populations in comparison to native areas. For each site, three sets of 30 Sherman traps were set out in the late evening in 10 meter x 10 meter grids with bait made from peanut butter, soy wax, rolled oats, peanut butter powder, raisins, and wild bird seeds. The traps were then checked 12-16 hours afterward for rodents and were reset again in the evening. This was repeated for three days in order to allow the rodents to habituate to the traps and to determine capture-recapture rates. During the first summer, two sampling sessions were conducted four weeks apart. The next summer, Catherine Grady et al, completed one sampling session with a greater number of sites.

After a successful trap, rodents were anesthetized with isopropanol and ear tagged for identification and for capture-recapture. Subsequently, body measurements, sex, and age were recorded. Blood, fecal, saliva, and external parasite samples were also collected. Blood collection was conducted using submandibular vein or saphenous

vein puncture. During the first summer, all rodents were released at the collection site after awakening from anesthesia. During the second summer on the third day of sampling, rodents were humanely euthanized following American Veterinary Medical Association guidelines. All rodent handling and sample collection was conducted with full body suit and N-95 mask protection. All contaminated surfaces were also sterilized with 5% microchem solution and ethanol after handling. After collecting all samples, species identification was confirmed for each captured rodent via cytochrome b PCR. Samples collected during the first summer used RNA extraction and Sin Nombre virus-specific, probe-based, q-RT PCR for hantavirus detection. Samples collected during the second summer were analyzed using a Sin Nombre virus-specific ELISA serology assay.

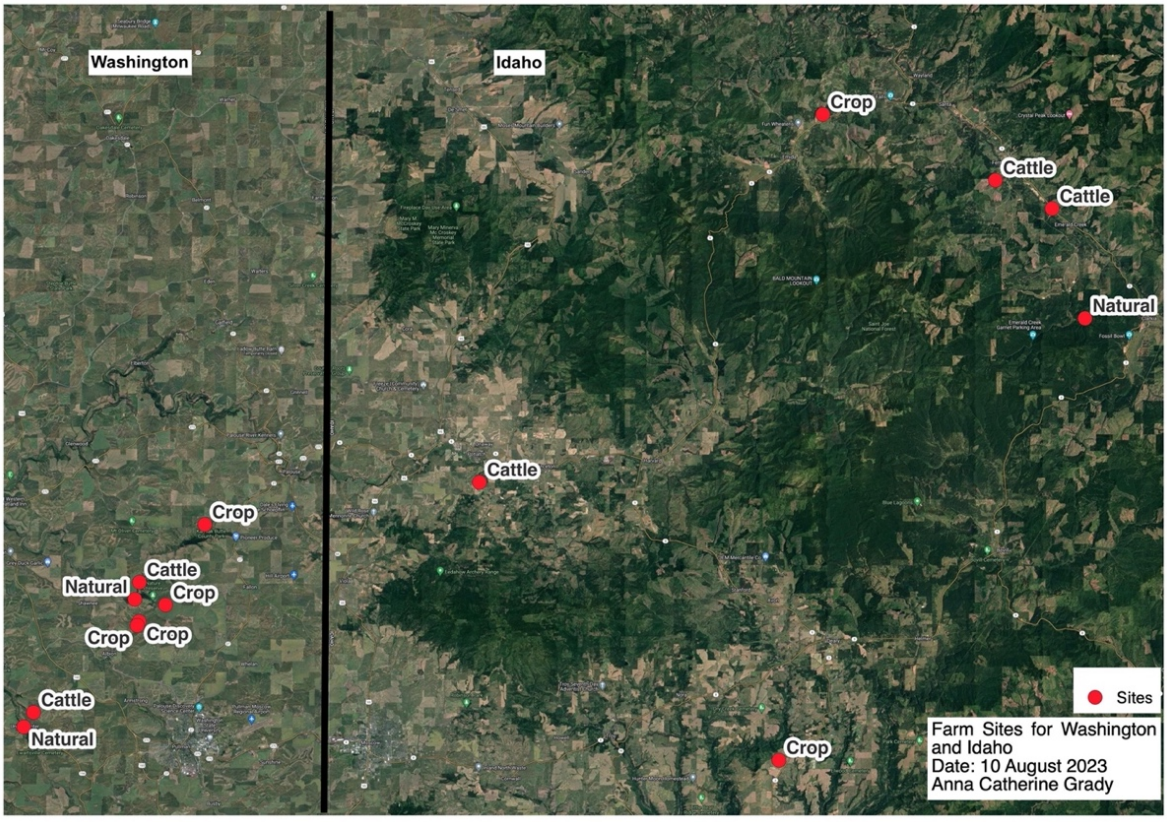

Figure 3: Sky view of the selected sites for sampling in Eastern Washington and Western Idaho

Results

A total of 208 rodents were caught and sampled throughout the two-year study. 102 were from sites that were more connected with natural landscape, and 106 were from sites in a more heterogeneous landscape that were better connected with agricultural activities. The most common rodent that was caught was *Peromyscus maniculatus*, the reservoir species for Sin Nombre virus. Other sampled species consisted of mouse, vole and chipmunk species such as *Neotamias minimus, Mus musculus, Tamias townsendii, Tamias amoenus, Lemmiscus curtatus, Microtus oregoni, Microtus pennsylvanicus, and Zapus princeps*. Samples from the first summer all tested negative for Sin Nombre virus q-RT PCR. Of 90 tested serum samples from 2023 (tested by Dr. Seifert using an enzyme-linked immunosorbent assay), 21 individuals tested seropositive for exposure to SNV nucleocapsid protein.

Conclusion

During the first summer, we did not find any q-RT PCR positive samples; however, only seven sites and 87 rodents were sampled, which does not provide enough information about the Palouse to draw conclusions. Previous studies investigating hantavirus prevalence among mouse populations in the United States have sampled a significantly higher number of rodents. For example, one study conducted in Montana sampled 390 rodents over two years at two separate sites (40), and another captured 426 rodents at two sites in California over the course of five years (41). It is also likely that hantavirus prevalence in the Palouse is concentrated in specific

patches based on resource abundance and habitat preference of deer mice, rather than evenly distributed across the region. During the second summer, 119 rodents were captured, and hantavirus detection was conducted via serology. These samples yielded several positive samples. Of those samples, significantly higher mouse seroprevalence was observed in crop and cattle areas than in natural habitats (Figure 4). This supports the hypothesis that agricultural activity may positively correlate with hantavirus prevalence. This is likely due to higher numbers of rodents in the same area, and subsequent rodent-to-rodent transmission of hantavirus. These findings may have implications for future hantavirus studies and may help to uncover distribution patterns of hantaviruses in other agricultural regions in the United States.

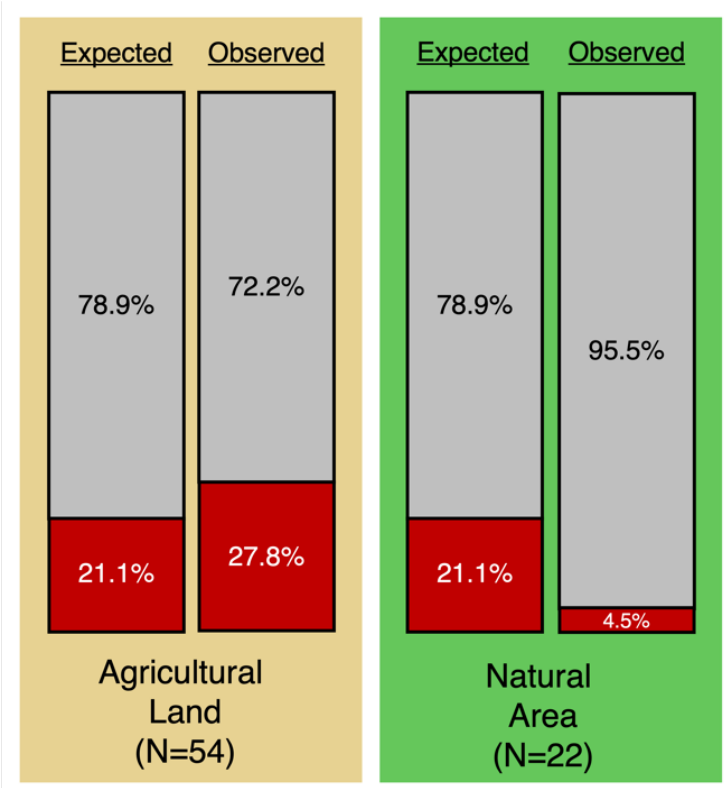

Figure 4: Results of a Fisher's Exact test on anti-SNV nucleocapsid protein seroprevalence in a subset of PEMA samples from 2023. p-value = 0.02943

Part Three: Developing *in vitro* Tools for the Study of Hantaviruses

Background

Our knowledge of hantavirus biology and tropism is also severely limited, which has impacted our ability to develop vaccinations and treatments for hantavirus-related diseases. One of the reasons for this is the lack of *in vitro* tools to study and recover wildtype virus. In order to better understand how hantaviruses work on a cellular level, it is essential to mimic natural virus-host interactions in a controlled environment. These studies would allow for observation and analysis of hantavirus behavior, which may then lead to the development of strategies to inhibit virus replication and transmission. Currently, laboratory studies of hantaviruses are rarely able to accomplish this. In fact, many current isolates of Sin Nombre virus that are available for research were isolated many years ago and have been regularly grown on Vero E6 cells, which are derived from the African green monkey. As the Vero-E6 cell line is defective in the interferon pathway, Vero-adapted isolates of Sin Nombre virus are unlikely to be representative of hantaviruses circulating in wild rodents.

To address this aspect of hantavirus research, the Lab of Function Viromics and Molecular Ecology and Zoonotic Pathogens Lab at Washington State University Paul G Allen School for Global Health have been collaborating to develop novel cell lines that can be used for hantavirus growth and study. The goal of this project is to create new tools that can help researchers grow hantaviruses under conditions that mimic virus replication in reservoir species. In order to do this, hantavirus reservoir species were first selected as source species to isolate and grow cells *in vitro*. Two species were

selected for cell propagation: *Peromyscus maniculatus* (PEMA) which is the primary reservoir species for Sin Nombre virus in North America, and *Carollia perspicillata* (CAP) which has been shown to harbor Araraquara virus. Hantavirus growth on PEMA cells has been attempted before unsuccessfully, but this study differed in that the cells were isolated from fetal mouse tissue, which lack a strong antiviral immune response. This is the first report of primary cells generated *from Carollia perspicillata* bats.

Methods

Isolation and characterization of cell lines

Frozen aliquots of tissue derived from target host species were shipped to the Lab of Functional Viromics from collaborators at Rocky Mountain Labs in Montana and Washington State University Vancouver. Isolated cell types included brain and kidney tissue from *P. maniculatus,* and brain, kidney, and lung tissue from *C. perspicillata*. Tissue was first degraded enzymatically with trypsin and with physical grinding to break up tissues and release individual cells. Separated cells were then distributed to several cell culture flasks in DMEM F12 media supplemented with antibiotics, non-essential amino acids, alpha-ketoglutarate, antifungal agent, sodium pyruvate, and 12% fetal bovine serum (FBS). Over the next several days, media was continuously replaced, and cells were observed for growth.

Once cells had sufficiently expanded, they were detached from their flasks with trypsin and diluted to eight cells/mL in media. This dilution was then distributed to three 96 well plates, 100 µL per well. In this format, zero to two cells were placed in separate wells. These individual cells were then observed over several days for morphology and

ability to divide. The cells that were best able to grow were selected for expansion into 6-well plates and cell culture flasks. These cells were then characterized for growth kinetics, transfectability, and survival. Growth kinetics and survival were measured by maintaining cell lines in cell culture flasks and noting the average confluency increase each day. The maximum confluency of each cell line was also noted, in addition to the maximum number of passages each cell line could undergo before the cells stopped dividing. Transfectability was observed by first cloning and expanding three plasmids, each expressing a different fluorescent molecule. All three plasmids were then combined and diluted to six different concentrations. These dilutions were used to transfect cells using polyethylene in a 24-well plate format. Expression of fluorescent molecules was then observed using fluorescence microscopy 24 and 48 hours post transfection.

Analysis of viral entry into novel cell lines

After initial characterization, a panel of vesicular stomatitis virus (VSV) pseudotype particles were made to mimic hantavirus cellular entry. Briefly, six hantavirus glycoprotein plasmids were cloned and propagated in *E coli*, after which they were used to transfect 293T cells. VSV particles lacking the glycoprotein gene were then used to infect the transfected cells. During budding, VSV particles acquired the expressed glycoproteins expressed on the cell surface, creating a replication incompetent VSV particle with hantavirus glycoproteins (Figure 5). These particles were used to infect novel cell lines, and viral entry was measured using a luciferase reporter assay. Four Old World hantavirus pseudotypes (Hantaan, Dobrava, Puumala, and

Seoul virus) and two New World hantavirus pseudotypes (Sin Nombre and Andes virus) were tested. The most promising cell line candidates were then taken for further development such as immortalization and wildtype virus infection. Dr. Letko followed up on these experiments by repeating the hantavirus entry assays on primary cells and immortalizing CAP kidney and brain cell lines using Cas9-mediated knockout of the p53 gene. Dr. Letko also completed a viral entry assay on these immortalized cells.

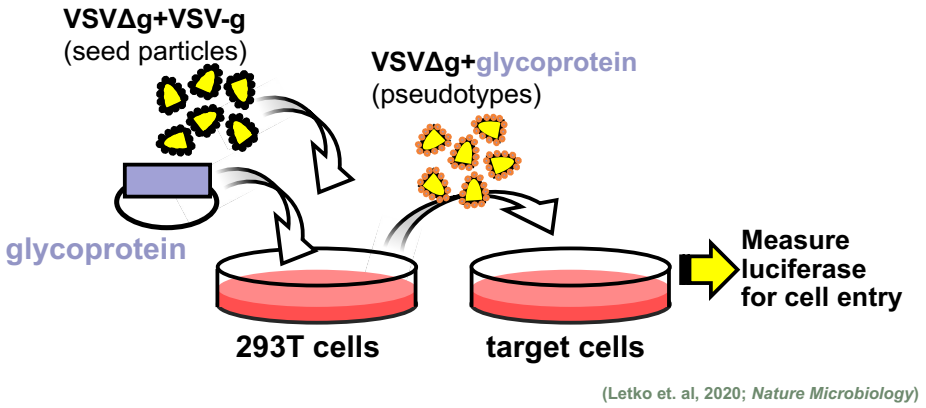

Figure 5: Visual representation of VSV pseudo type production. Plasmids encoding the glycoprotein of the target virus are used to transfect 293T cells, after which VSV particles lacking a glycoprotein gene are used to infect these cells. This produces VSV pseudotypes bearing the glycoprotein of the target virus, which also produces genetic information encoding green fluorescent protein and luciferase.

Growth of full hantavirus on novel cell lines

Two cell lines were selected as promising candidates for hantavirus growth: immortalized CAP kidney cells and primary PEMA kidney cells. These cell lines were then infected with wildtype hantavirus in a biosafety level 3 (BSL3) environment. Briefly, cells were plated in a 6-well format and transported to a BSL3 laboratory. Hantaviruses, including an isolate of Sin Nombre virus from the Center of Disease Control (CDC SNV), and four q-RT PCR-positive field samples, were then thawed and diluted. Two

mL diluted virus was then added to each well of plated cells and centrifuged at low speed for one hour. Supernatant was then removed, and media was replaced with 2% FBS media. At days 0, 8, and 13, 50 µL of supernatant was taken from each well of infected cells and diluted in 175 µL DNA/RNA shield. After day 13, the remaining volume in each well was transferred to a new tube and frozen at -80 degrees Celsius. The samples diluted in DNA/RNA shield were used for magnetic bead RNA extraction, and detection of Sin Nombre virus was completed using probe-based, Sin Nombre virus specific, q-RT PCR.

Detection of cytopathic effect

In a follow-up experiment, the same cells were infected with CDC SNV and Hantaan virus as described above. On days 8 and 13, cells were visualized under the microscope for cytopathic effect. Images were captured and results were recorded for each well of infected cells.

Results

Isolation and characterization of cell lines

Tissue was successfully degraded into individual cells, most of which were unable to grow. However, there were populations of fibroblasts that grew quite quickly. Initially, many cell types and morphologies were distinguishable within each cell culture flask. However, after single cell clones were separated, homogenous cell monolayers began to grow with consistency. PEMA brain cells showed a thin, branching morphology. These cells created a weblike structure and were typically evenly spaced

in the flask. PEMA kidney cells were much more compact and smaller, creating pockets of dense cell monolayers that expanded into each other (Figure 6). CAP brain cells also showed a branching morphology but were more compact that PEMA brain cells. CAP kidney cells grew quite well and were also very compact and grid-like. CAP lung cells grew in close proximity to each other, and had a large, curved morphology (Figure 7).

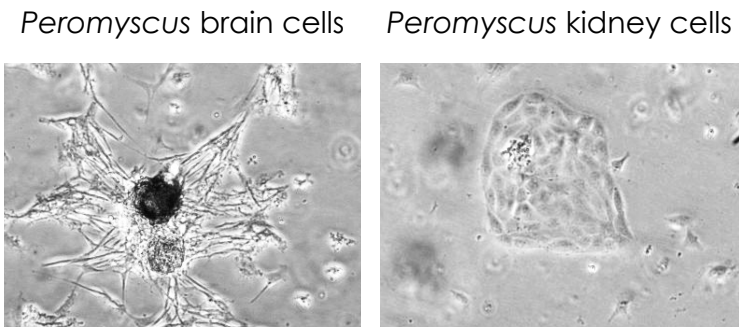

Figure 6: Images of cells isolated from brain and kidney tissue of *Peromyscus maniculatus.*

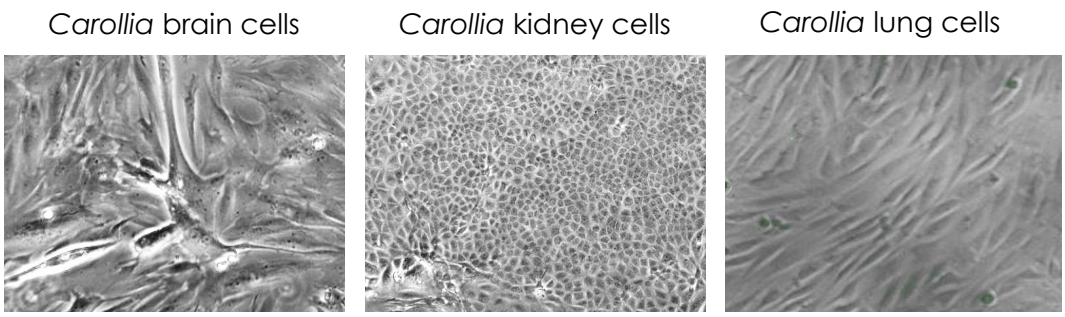

Figure 7: Images of cells isolated from lung, brain and kidney tissue of *Carollia perspicillata*

Both PEMA brain and kidney cells were able to grow to full confluency. However, PEMA kidney cells were able to grow significantly faster and survive longer. On the other hand, PEMA brain cells grew very slowly but were more transfectable than kidney cells (Figure 8). CAP cells differed from PEMA cells in that they grew quickly and were able to survive several passages. Among the CAP cells, the kidney and lung cells grew

the fastest. However, the kidney cells grew to a greater confluency and survived for a longer time. The brain cells grew at a slower rate and did not survive very long. All cells were equally transfectable (Figure 9).

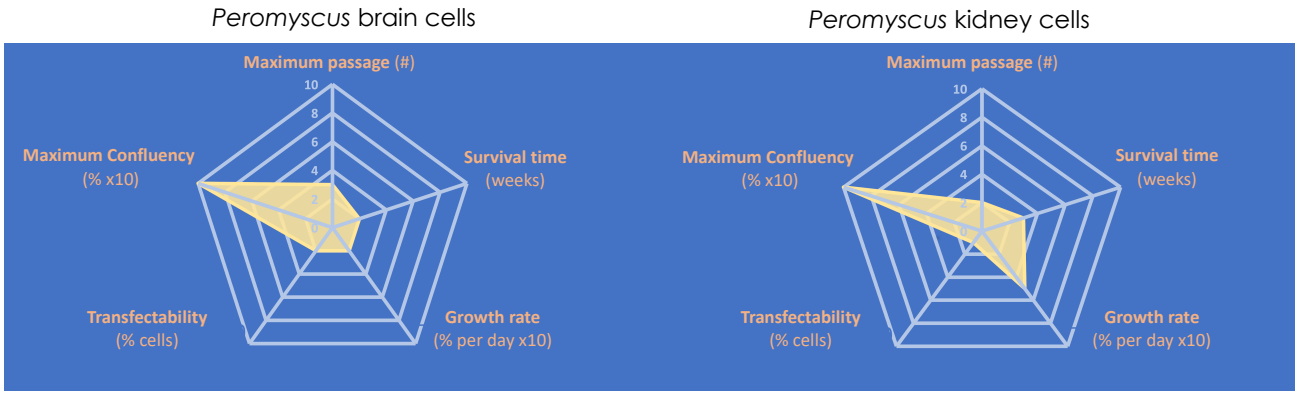

Figure 8: Characteristics of novel cell lines derived from *Peromyscus maniculatus*. Radar plots describe maximum passage number cell line can survive, the survival time (in weeks), maximum confluency (expressed as a percentage, multiplied by 10), growth rate (expressed in percent confluency increased per day, multiplied by 10), and transfectability (expressed in the percentage of cells that express transfected markers).

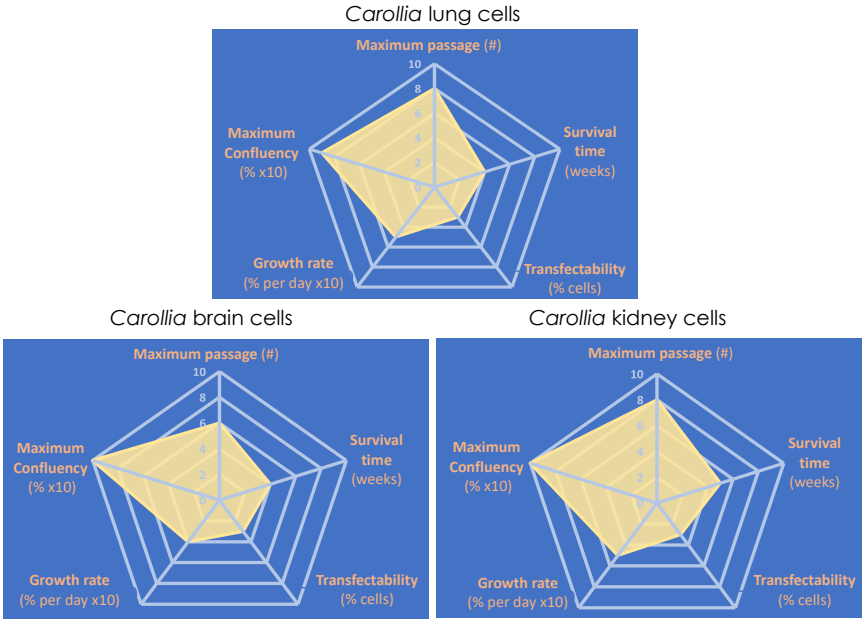

Figure 9: Characteristics of novel cell lines derived from *Carollia perspicillata*. Radar plots describe maximum passage number cell line can survive, the survival time (in weeks), maximum confluency (expressed as a percentage, multiplied by 10), growth rate (expressed in percent confluency increased per day, multiplied by 10), and transfectability (expressed in the percentage of cells that express transfected markers).

Analysis of viral entry into novel cell lines

Viral entry behavior was analyzed in all primary cell types and in immortalized CAP cells. In primary PEMA cells, both the brain and kidney cells were permissive to cellular entry by all six tested hantavirus pseudotypes. In fact, cellular entry was similar to that of Vero cells, the standard cell line that is currently used in most hantavirus research. Notably, the PEMA kidney cells were more permissive to infection by all hantaviruses than the PEMA brain cells, particularly for Sin Nombre virus (Figure 10). Primary CAP cells were also permissive to entry from all six hantavirus pseudotypes. However, entry was not as successful as in PEMA cells or in Vero cells. Primary CAP cells were most permissive to New World hantavirus pseudotypes, and kidney/lung cells were most permissive to Old World hantavirus pseudotypes (Figure 11). Interestingly, the viral entry assays conducted on the immortalized version of the CAP cells yielded very positive results. Viral entry was significantly boosted compared to the experiments done with primary cells. Notably, both immortalized cell types were very permissive to Dobrava, Hantaan, and Andes virus. The immortalized CAP brain cells were also very permissive to Sin Nombre virus pseudotypes, and performed similarly to Vero cells for all six hantavirus pseudotypes (Figure 12).

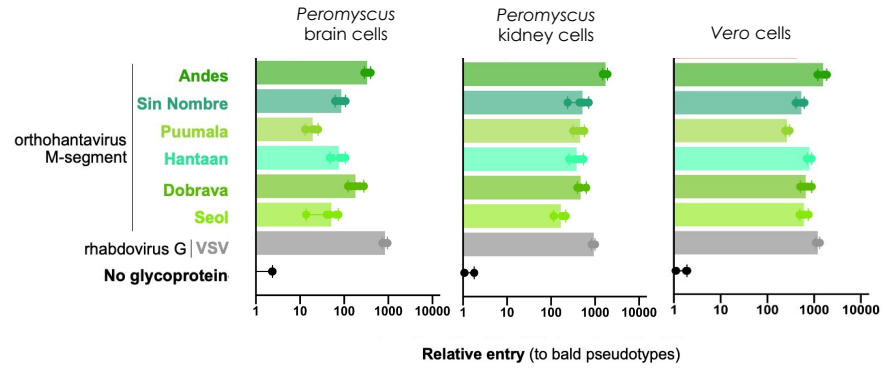

Figure 10: Viral entry phenotypes on primary cells derived from *Peromyscus maniculatus*. All cell types were permissive to all six hantavirus pseudotypes.

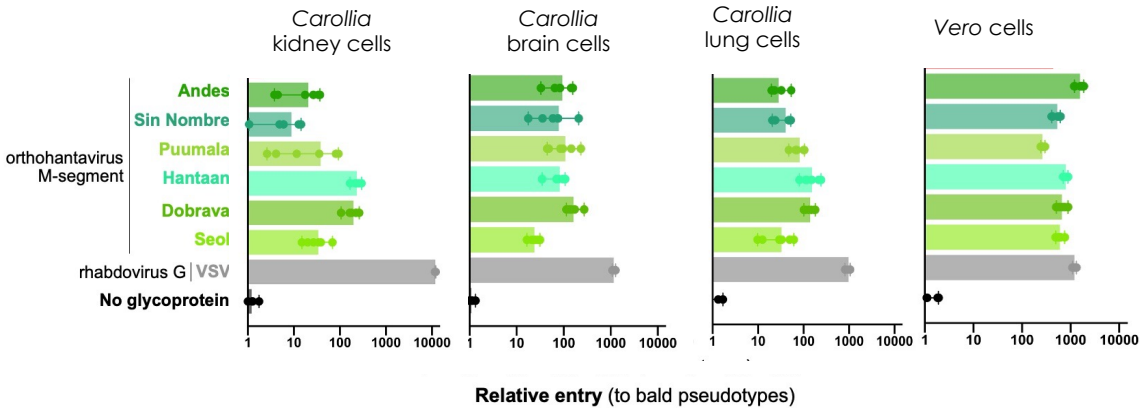

Figure 11: Viral entry phenotypes on primary cells derived from *Carollia perspicillata*. All cell types were permissive to all six hantavirus pseudotypes.

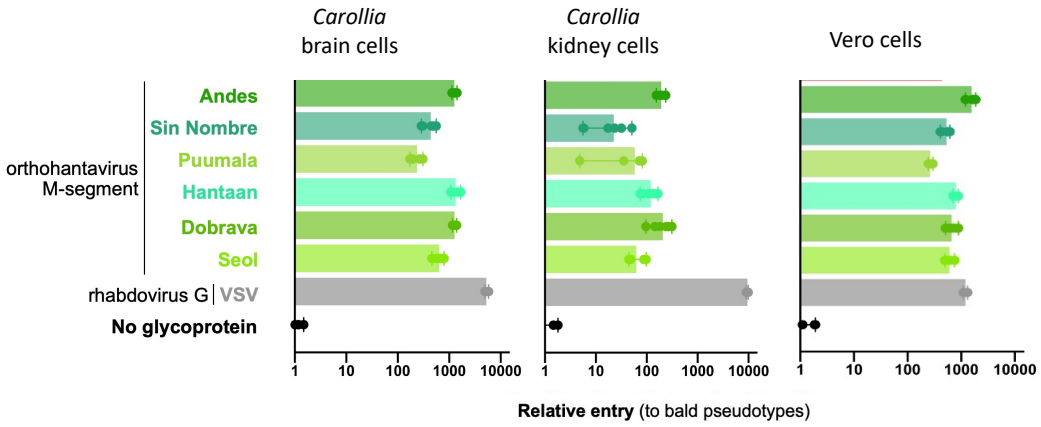

Figure 12: Viral entry phenotypes on immortalized cells derived from *Carollia perspicillata*. All cell types were permissive to all six hantavirus pseudotypes, and entry was more successful than what was observed in primary cell lines derived from the same species.

Growth of full hantavirus on novel cell lines

Complete hantaviruses were used to infect three different cell lines, after which Cq values from q-RT PCR data was used to estimate relative concentrations of Sin Nombre virus grown on each cell type. After analyzing q-RT PCR data, it was found that PEMA kidney cells, but not immortalized CAP kidney cells, were able to grow SNV CDC. However, the observed growth was not as pronounced as in Vero cells (Figure 13). For three of the four tested field samples, virus growth failed on all three cell lines. However, q-RT PCR data indicated that the third field sample may have grown on immortalized CAP kidney cells, but not PEMA or Vero cells (Figure 14).

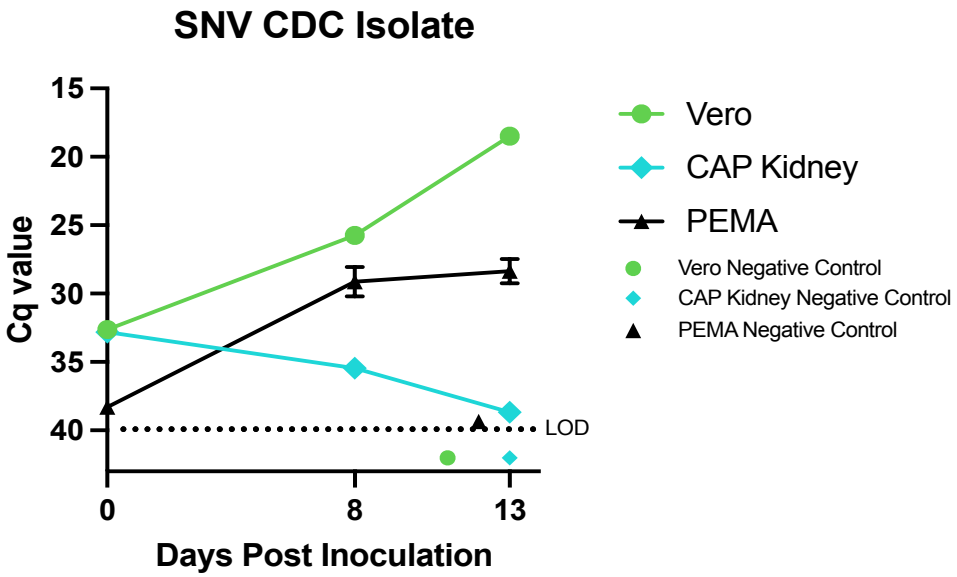

Figure 13: Growth curve of Sin Nombre virus isolate supplied by the CDC (SNC CDC) on primary PEMA kidney cells, immortalized CAP kidney cells, and Vero cells, expressed as Cq values from q-RT PCR. SNV CDC grew successfully on PEMA and Vero cells, but not on CAP cells. Negative controls were at or below the limit of detection (LOD).

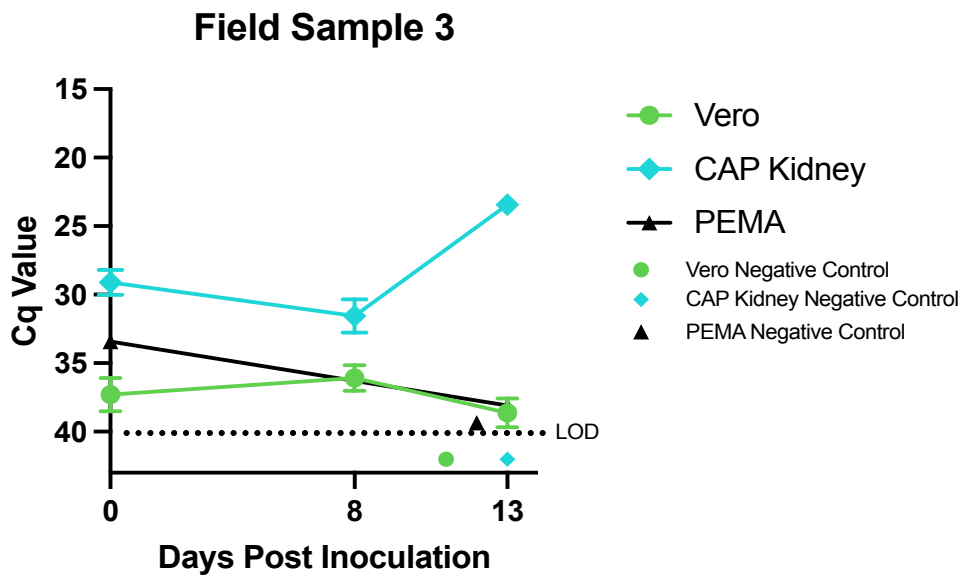

Figure 14: Growth curve of Sin Nombre virus field sample on primary PEMA kidney cells, immortalized CAP kidney cells, and Vero cells, expressed as Cq values from q-RT PCR. Field sample grew on immortalized CAP kidney cells, but not on PEMA cells or Vero cells. Negative controls were at or below the limit of detection (LOD).

Detection of cytopathic effect

During another experiment in the BSL3 laboratory, immortalized CAP kidney cells were infected with Hantaan virus. To check for cytopathic effect associated with virus infection and cellular destruction, images of cell monolayers were captured on days 8 and 13. On both days, visible cytopathic effect was apparent on the immortalized CAP kidney cells, which is rarely seen in hantavirus infections (Figure 15). This may indicate that Hantaan virus is able to successfully replicate on these cells.

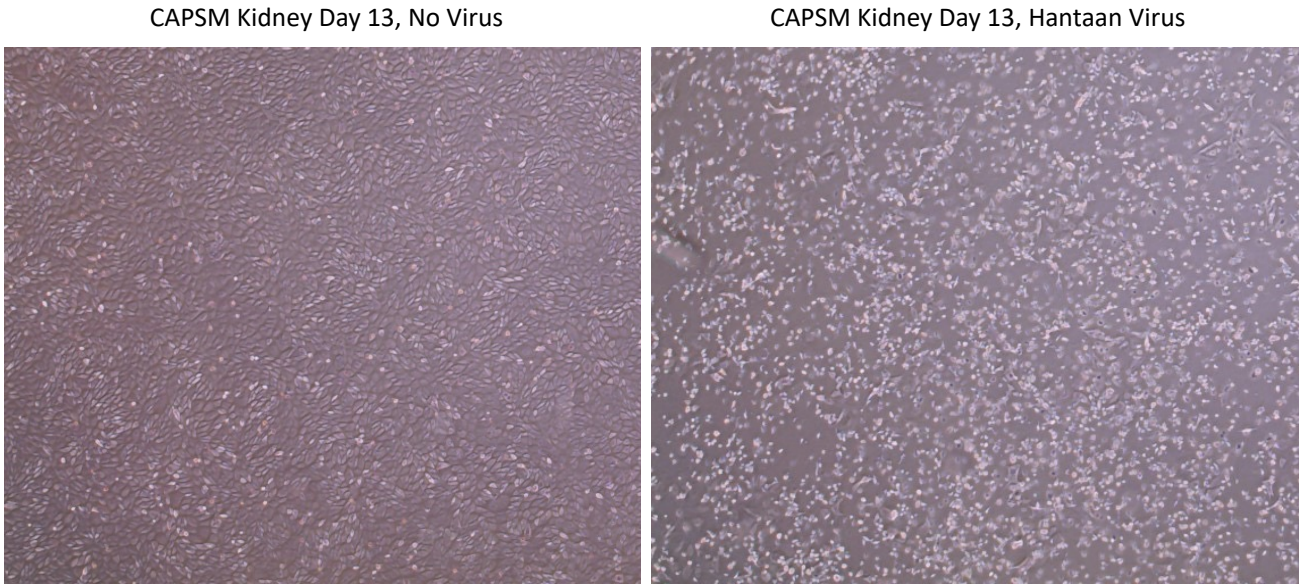

Figure 15: Observed CPE in immortalized CAP kidney cells after 13 days of Hantaan virus infection.

Conclusion

As a result of these experiments, several different cell lines have been developed or are currently in development. For many of these cells, promising data have been produced supporting the hypothesis that these cells are permissive to hantavirus infection and can grow several different kinds of hantaviruses in the lab. As this work progresses, it is our hope that many of these cell lines will be used by researchers around the world, and that they may reliably enable us to study natural virus-host interactions and recover hantavirus isolates from the field and the clinic. Such work is vital for the development of hantavirus vaccines and treatments, especially for New World hantaviruses, which pose a greater threat to human health and cannot currently be treated.

Acknowledgements

I would like to thank my research mentors, Dr. Michael Letko, Dr. Alan Goodman, and Dr. Stephanie Seifert, for all of their support and assistance throughout my research journey. I would also like to thank all of the participating laboratory members of the Lab of Functional Viromics and the MEZAP lab for their contributions to this continuing work. Thank you!

Lab of Functional Viromics – Dr. Michael Letko, Dr. Mitra Mizanani

Molecular Ecology and Zoonotic Pathogens lab – Dr. Stephanie Seifert, Dr. Pilar Fernandez, Catherine Grady (MSc candidate)

Washington State University Vancouver

Rock Mountain Labs (NIH)

References

1 - de Oliveira RC, Guterres A, Fernandes J, D'Andrea PS, Bonvicino CR, de Lemos ER. Hantavirus reservoirs: current status with an emphasis on data from Brazil. Viruses. 2014 Apr 29;6(5):1929-73. doi: 10.3390/v6051929. PMID: 24784571; PMCID: PMC4036540.

2 - Alonso DO, Pérez-Sautu U, Bellomo CM, Prieto K, Iglesias A, Coelho R, Periolo N, Domenech I, Talmon G, Hansen R, Palacios G, Martinez VP. Person-to-Person Transmission of Andes Virus in Hantavirus Pulmonary Syndrome, Argentina, 2014. Emerg Infect Dis. 2020 Apr;26(4):756-759. doi: 10.3201/eid2604.190799. PMID: 32186494; PMCID: PMC7101103.

3 - Prist PR, Uriarte M, Fernandes K, Metzger JP. Climate change and sugarcane expansion increase Hantavirus infection risk. PLoS Negl Trop Dis. 2017 Jul 20;11(7):e0005705. doi: 10.1371/journal.pntd.0005705. PMID: 28727744; PMCID: PMC5519001.

4 - Singh S, Numan A, Sharma D, Shukla R, Alexander A, Jain GK, Ahmad FJ, Kesharwani P. Epidemiology, virology and clinical aspects of hantavirus infections: an overview. Int J Environ Health Res. 2022 Aug;32(8):1815-1826. doi: 10.1080/09603123.2021.1917527. Epub 2021 Apr 22. PMID: 33886400.

5 - Mittler E, Dieterle ME, Kleinfelter LM, Slough MM, Chandran K, Jangra RK. Hantavirus entry: Perspectives and recent advances. Adv Virus Res. 2019;104:185-224. doi: 10.1016/bs.aivir.2019.07.002. Epub 2019 Aug 7. PMID: 31439149; PMCID: PMC6881143.

6 – Center for Disease Control and Prevention. (2017, January 18). CDC – hantavirus. https://www.cdc.gov/hantavirus/index.html

7 - Vial PA, Ferrés M, Vial C, Klingström J, Ahlm C, López R, Le Corre N, Mertz GJ. Hantavirus in humans: a review of clinical aspects and management. Lancet Infect Dis. 2023 Sep;23(9):e371-e382. doi: 10.1016/S1473-3099(23)00128-7. Epub 2023 Apr 24. PMID: 37105214.

8 - Wei X, Li X, Song S, Wen X, Jin T, Zhao C, Wu X, Liu K, Shao Z. Trends and focuses of hantavirus researches: a global bibliometric analysis and visualization from 1980 to 2020. Arch Public Health. 2022 Oct 1;80(1):218. doi: 10.1186/s13690-022-00973-5. Erratum in: Arch Public Health. 2022 Nov 17;80(1):236. PMID: 36182906; PMCID: PMC9526533.

9 - Firth C, Tokarz R, Simith DB, Nunes MR, Bhat M, Rosa ES, Medeiros DB, Palacios G, Vasconcelos PF, Lipkin WI. Diversity and distribution of hantaviruses in South America. J Virol. 2012 Dec;86(24):13756-66. doi: 10.1128/JVI.02341-12. Epub 2012 Oct 10. PMID: 23055565; PMCID: PMC3503106.

10 - Jonsson CB, Figueiredo LT, Vapalahti O. A global perspective on hantavirus ecology, epidemiology, and disease. Clin Microbiol Rev. 2010 Apr;23(2):412-41. doi: 10.1128/CMR.00062-09. PMID: 20375360; PMCID: PMC2863364.

11 - Bueno LM, Melo DM, Azevedo RD, de Souza WM, Figueiredo LTM. Serological evidence of hantavirus infection in neotropical bats in an urban area of São Paulo State, Brazil. Trans R Soc Trop Med Hyg. 2023 Apr 3;117(4):297-300. doi: 10.1093/trstmh/trac111. PMID: 36477881; PMCID: PMC10069298.

12 - Sabino-Santos G Jr, Maia FGM, Martins RB, Gagliardi TB, Souza WM, Muylaert RL, Luna LKS, Melo DM, Cardoso RS, Barbosa NDS, Pontelli MC, Mamani-Zapana PR, Vieira TM, Melo NM, Jonsson CB, Goodin D, Salazar-Bravo J, daSilva LLP, Arruda E, Figueiredo LTM. Natural infection of Neotropical bats with hantavirus in Brazil. Sci Rep. 2018 Jun 13;8(1):9018. doi: 10.1038/s41598-018-27442-w. PMID: 29899544; PMCID: PMC5998146.

13 - Avšič-Županc T, Saksida A, Korva M. Hantavirus infections. Clin Microbiol Infect. 2019 Apr;21S:e6-e16. doi: 10.1111/1469-0691.12291. Epub 2015 Jun 22. PMID: 24750436.

14 - Zhang YZ. Discovery of hantaviruses in bats and insectivores and the evolution of the genus Hantavirus. Virus Res. 2014 Jul 17;187:15-21. doi: 10.1016/j.virusres.2013.12.035. Epub 2014 Feb 6. PMID: 24509342.

15 - Liu R, Ma H, Shu J, Zhang Q, Han M, Liu Z, Jin X, Zhang F, Wu X. Vaccines and Therapeutics Against Hantaviruses. Front Microbiol. 2020 Jan 30;10:2989. doi: 10.3389/fmicb.2019.02989. PMID: 32082263; PMCID: PMC7002362.

16 - Rupasinghe S, Bowattage S, Herath L, Rajaratnam A. Two Atypical Cases of Hantavirus Infection: Experience from a Tertiary Care Unit in Sri Lanka. Case Rep Infect Dis. 2021 Apr 21;2021:5555613. doi: 10.1155/2021/5555613. PMID: 33976946; PMCID: PMC8084661.

17 - Yotsuyanagi H, Koike K, Meng G, Yasuda K, Ogata I, Kimura S, Ohkubo A. Acute exacerbation of autoimmune liver disease associated with hantaviral infection. Scand J Infect Dis. 1998;30(1):81-3. doi: 10.1080/003655498750002358. PMID: 9670364.

18 - Yotsuyanagi H, Koike K, Meng G, Yasuda K, Ogata I, Kimura S, Ohkubo A. Acute exacerbation of autoimmune liver disease associated with hantaviral infection. Scand J Infect Dis. 1998;30(1):81-3. doi: 10.1080/003655498750002358. PMID: 9670364.

19 - Pastissier A, Humbert S, Naudion P, Meaux-Ruault N, Badoz M, Magy-Bertrand N. Severe Sinus Bradycardia in Puumala virus infection. Int J Infect Dis. 2019 Feb;79:75-76. doi: 10.1016/j.ijid.2018.11.019. Epub 2018 Nov 29. PMID: 30503652.

20 - Krumm P, Zitzelsberger T, Gawaz M, Greulich S. Young patient with hantavirus-induced myocarditis detected by comprehensive cardiac magnetic resonance assessment. BMC Infect Dis. 2019 Jan 6;19(1):15. doi: 10.1186/s12879-018-3658-8. PMID: 30612548; PMCID: PMC6322348.

21 - Rasmuson J, Lindqvist P, Sörensen K, Hedström M, Blomberg A, Ahlm C. Cardiopulmonary involvement in Puumala hantavirus infection. BMC Infect Dis. 2013 Oct 28;13:501. doi: 10.1186/1471-2334-13-501. PMID: 24160911; PMCID: PMC4231367.

22 - Hautala N, Partanen T, Kubin AM, Kauma H, Hautala T. Central Nervous System and Ocular Manifestations in Puumala Hantavirus Infection. Viruses. 2021 May 31;13(6):1040. doi: 10.3390/v13061040. PMID: 34072819; PMCID: PMC8229408.

23 - Vertigo - Ahlm C, Lindén C, Linderholm M, Alexeyev OA, Billheden J, Elgh F, Fagerlund M, Zetterlund B, Settergren B. Central nervous system and ophthalmic involvement in nephropathia epidemica (European type of haemorrhagic fever with renal syndrome). J Infect. 1998 Mar;36(2):149-55. doi: 10.1016/s0163-4453(98)80004-2. PMID: 9570645.

24 - Lo SH, Chen PT, Yu WJ, Hsieh KS, Chen TC. Case Report: Spinal Subarachnoid Hemorrhage: A Rare Complication of Hemorrhagic Fever with Renal Syndrome. Am J Trop Med Hyg. 2021 Feb 16;104(4):1432-1434. doi: 10.4269/ajtmh.20-0823. PMID: 33591937; PMCID: PMC8045668.

25 - Liu E, Lv S, Yi P, Feng L, Deng X, Xia H, Xu Y. Central nervous system infection with Seoul Orthohantavirus in a child after hematopoietic stem cell transplantation: a case report. Virol J. 2022 Apr 22;19(1):75. doi: 10.1186/s12985-022-01766-6. PMID: 35459229; PMCID: PMC9034594.

26 - Cerar D, Avsic-Zupanc T, Jereb M, Strle F. Case report: severe neurological manifestation of Dobrava hantavirus infection. J Med Virol. 2007 Dec;79(12):1841-3. doi: 10.1002/jmv.21021. PMID: 17935168.

27 - Talamonti L, Padula PJ, Canteli MS, Posner F, Marczeski FP, Weller C. Hantavirus pulmonary syndrome: encephalitis caused by virus Andes. J Neurovirol. 2011 Apr;17(2):189-92. doi: 10.1007/s13365-010-0011-4. Epub 2011 Jan 15. PMID: 21240581.

28 - Huisa BN, Chapin JE, Adair JC. Central nervous system complications following Hanta virus cardiopulmonary syndrome. J Neurovirol. 2009 Apr;15(2):202-5. doi: 10.1080/13550280802491485. PMID: 19089788.

29 - Fawcett SJ, Chen JS, Fawcett RW. Acute Hantavirus Infection Presenting With Fever and Altered Mentation in the Absence of Pulmonary or Renal Manifestations. Open Forum Infect Dis. 2022 Aug 29;9(9):ofac430. doi: 10.1093/ofid/ofac430. PMID: 36119963; PMCID: PMC9472660.

30 - Hopkins RO, Larson-Lohr V, Weaver LK, Bigler ED. Neuropsychological impairments following hantavirus pulmonary syndrome. J Int Neuropsychol Soc. 1998 Mar;4(2):190-6. doi: 10.1017/s1355617798001908. PMID: 9529829.

31 - Zhou Y, Yang J, Hai H, Dong J, Wen Y. Hantavirus infection-related acute inflammatory demyelinative polyradiculoneuropathy: A case report and literature review. Medicine (Baltimore). 2024 Mar 8;103(10):e37332. doi: 10.1097/MD.0000000000037332. PMID: 38457548; PMCID: PMC10919522.

32 - Lambin EF, Meyfroidt P. Global land use change, economic globalization, and the looming land scarcity. Proc Natl Acad Sci U S A. 2011 Mar 1;108(9):3465-72. doi: 10.1073/pnas.1100480108. Epub 2011 Feb 14. PMID: 21321211; PMCID: PMC3048112.

33 - Ecke F, Han BA, Hörnfeldt B, Khalil H, Magnusson M, Singh NJ, Ostfeld RS. Population fluctuations and synanthropy explain transmission risk in rodent-borne zoonoses. Nat Commun. 2022 Dec 7;13(1):7532. doi: 10.1038/s41467-022-35273-7. PMID: 36477188; PMCID: PMC9729607.

34 - Zuckerman, L. (2017, July 6). Outbreak of hantavirus infections kills three in Washington state. Reuters. https://www.reuters.com/article/idUSKBN19S0EJ/

35 - Associated Press (1993, December 21). New Test Show Idaho Teen Died of Hantavirus. Deseret News. https://www.deseret.com/1993/12/21/19082876/new-tests-show-idaho-teen-died-of-hantavirus/#:~:text=An%20Idaho%20teenager%20died%20in,developed%20severe%20respiratory%20problems%2C%20Dr

36 - McDonough, T. (1999, May 15). Hantavirus death sparks investigation. Moscow-Pullman Daily News. https://dnews.com/local/hantavirus-death-sparks-investigation/article_54b67ea4-f7af-5954-80e3-b2abfd0f0e87.html

37 - Ecke F, Han BA, Hörnfeldt B, Khalil H, Magnusson M, Singh NJ, Ostfeld RS. Population fluctuations and synanthropy explain transmission risk in rodent-borne zoonoses. Nat Commun. 2022 Dec 7;13(1):7532. doi: 10.1038/s41467-022-35273-7. PMID: 36477188; PMCID: PMC9729607.

38 - WhiteA.J., PoulinR.G., WisselB., DoucetteJ.L., and SomersC.M.. 2012. Agricultural land use alters trophic status and population density of deer mice (*Peromyscus maniculatus*) on the North American Great Plains. *Canadian Journal of Zoology*. **90**(7): 868-874. https://doi.org/10.1139/z2012-055

39 - Berl JL, Kuenzi AJ, Flaherty EA, Swihart RK. INTERSPECIFIC COMPARISON OF HANTAVIRUS PREVALENCE IN PEROMYSCUS POPULATIONS FROM A FRAGMENTED AGRO-ECOSYSTEM IN INDIANA, USA. J Wildl Dis. 2018 Jan;54(1):147-150. doi: 10.7589/2017-02-022. Epub 2017 Oct 4. PMID: 28977768.

40 - Williamson BN, Meade-White K, Boardman K, Schulz JE, Telford CT, Figueroa Acosta DM, Bushmaker T, Fischer RJ, Rosenke K, Feldmann H. Continuing Orthohantavirus Circulation in Deer Mice in Western Montana. Viruses. 2021 May 27;13(6):1006. doi: 10.3390/v13061006. PMID: 34072112; PMCID: PMC8226622.

41 - Danforth ME, Messenger S, Buttke D, Weinburke M, Carroll G, Hacker G, Niemela M, Andrews ES, Jackson BT, Kramer V, Novak M. Long-Term Rodent Surveillance after Outbreak of Hantavirus Infection, Yosemite National Park, California, USA, 2012. Emerg Infect Dis. 2020 Mar;26(3):560-567. doi: 10.3201/eid2603.191307. PMID: 32091360; PMCID: PMC7045852.